Journal of Power Sources 194 (2009) 526–530

Contents lists available at ScienceDirect

Journal of Power Sources

journal homepage: www.elsevier.com/locate/jpowsour

Short communication

High voltage spinel cathode materials for high energy density and high rate capability Li ion rechargeable batteries

Rajesh K. Katiyar[a], Rahul Singhal[b], Karina Asmar[b], Ricky Valentin[a], Ram S. Katiyar[b,*]

[a] Department of Mechanical Engineering, University of Puerto Rico, Mayaguez, PR 00681, USA
[b] Department of Physics and Institute for Functional Nanomaterials, University of Puerto Rico, San Juan, PR 00931-3343, USA

ARTICLE INFO

Article history:
Received 30 April 2009
Received in revised form 10 May 2009
Accepted 12 May 2009
Available online 21 May 2009

Keywords:
High energy density
High voltage
Li ion batteries
Rate capability
Cathode
$LiMn_2O_4$

ABSTRACT

We have synthesized $LiMn_{1.5}Ni_{0.4}Cr_{0.1}O_4$ cathode material for high energy density Li ion rechargeable batteries using sol–gel method. The synthesized materials were characterized using X-ray diffraction (XRD), X-ray photoelectron spectroscopy, cyclic voltammetry and charge–discharge characteristics. It was found that phase pure materials were obtained an annealing temperature of 875 °C for 15 h. The maximum discharge capacity at a constant charge–discharge current rate 1*C*, 0.5*C*, and 0.2*C* were found to be about 99 mAh g^{-1}, 110 mAh g^{-1}, and 131 mAh g^{-1}, respectively. The capacity retentions after 50 charge–discharge cycles were found to be about 99%, 97%, and 97.3% at discharge current rates of 0.2*C*, 0.5*C*, and 1*C*. The stable electrochemical behavior of the above cathode material even at high *C* rate, showed that it could be used for high energy density and high rate capability Li ion rechargeable batteries.

1. Introduction

Due to increased demand of high energy density batteries and high power density batteries for light vehicle, and HEV applications, the research towards finding new cathode materials for rechargeable Li ion batteries has been accelerated [1–4]. The important key factors for considerations are low price, echo friendly, prolonged cycle life, safe operation, and high specific energy. The high energy density materials can be achieved by either increasing discharge capacity of the cathode or increasing the working potential of the cathode materials [5]. In spinel $LiMn_2O_4$ structure the maximum theoretical discharge capacity is 148 mAh g^{-1} and experimentally, its initial discharge capacity in 4 V range is about 130 mAh g^{-1}, with large capacity fading upon cycling [6–8]. It has been reported by several researchers that the high voltage spinel oxides with composition $LiMn_{2-x}M_xO_4$ (M = Ni, Cr, Co, Cu, or any other transition metal element) have remarkable properties, such as high potential, high energy density, and high rate capability [9–11].

Yoon et al. [9] synthesized $LiM_{0.5}Mn_{1.5}O_4$ (M = Ni, Co, Cr) cathode materials by solid state route. They found that these materials showed a discharge plateau around 5 V. The $LiMn_{1.5}Ni_{0.5}O_4$, $LiMn_{1.5}Co_{0.5}O_4$, $LiMn_{1.5}Cr_{0.5}O_4$, cathode materials showed an initial discharge capacity of 123 mAh g^{-1}, 130 mAh g^{-1}, and 140 mAh g^{-1}. They performed maximum 10 charge–discharge cycles of these materials with considerable capacity fading upon cycling.

Recently, it has been investigated that $LiMn_{1.5}Ni_{0.5}O_4$ cathode materials could be used up to 4.7 V range. Wei et al. synthesized [10] $LiMn_{2-x}Ni_xO_4$ ($0 \le x \le 0.5$) spinel cathode materials. They found that as the concentration of Ni increases from 0.0 to 0.5, the discharge plateau around 4.7 V increases and the plateau around 4.1 V decreases because of the change is the oxidation state of Mn^{3+} and Ni^{2+} upon increased Ni concentration. We have synthesized [11] $LiMn_{2-x}Ni_xO_4$ cathode materials by sol–gel method. The Ni concentration varies as 0.125, 0.250, 0.375, and 0.50. We found that as the nickel concentration increases, the initial discharge capacity increases. The maximum discharge capacity was found as 140.18 mAh g^{-1} for $LiMn_{1.5}Ni_{0.5}O_4$. The discharge capacity retention was found to be about 98% after 50 charge–discharge cycles.

It has been reported by several researchers that Cr doped spinels could be used for 5 V application [12–14]. Rajakumar et al. [12] synthesized multiple doped spinels, $LiM_{0.25}Ni_{0.25}Mn_{1.5}O_4$ (M = Cr, Fe, and Co) via glycine assisted sol–gel method. The initial discharge capacities of $LiCr_{0.25}Ni_{0.25}Mn_{1.5}O_4$, $LiFe_{0.25}Ni_{0.25}Mn_{1.5}O_4$, and $LiCo_{0.25}Ni_{0.25}Mn_{1.5}O_4$ were reported as 116 mAh g^{-1}, 120 mAh g^{-1}, and 80 mAh g^{-1}, respectively. They reported that $LiFe_{0.25}Ni_{0.25}Mn_{1.5}O_4$ cathode material showed the best electrochemical performance upon cycling, where the capacity fading was observed as 0.05 mAh g^{-1} $cycles^{-1}$, for 20 charge–discharge cycles. Suryakala et al. [13] synthesized $LiMn_{2-x}Cr_xO_4$ cathode materials by sol–gel method. They observed discharge plateau in 5 V region

* Corresponding author. Tel.: +1 787 751 4210.
E-mail address: rkatiyar@uprrp.edu (R.S. Katiyar).

0378-7753/$ – see front matter © 2009 Elsevier B.V. All rights reserved.
doi:10.1016/j.jpowsour.2009.05.017

and found the discharge capacity increases upon increasing Cr concentration. The initial discharge capacity for 0.1, 0.2, 0.3, and 0.4 Cr doping was found to be about 128 mAh g^{-1}, 131 mAh g^{-1}, 140 mAh g^{-1}, and 142 mAh g^{-1}, respectively. They, however, did not report any cycleability data. Yi et al. [14] reported electrochemical performance of $LiMn_{1.4}Cr_{0.2}Ni_{0.4}O_4$ cathode materials in the 4 V range. They found that at a charge–discharge rate of 0.2*C*, the cathode materials showed an initial discharge capacity of about 130.8 mAh g^{-1} in the voltage range of 3.3–4.95 V. After 50 charge–discharge cycles the discharge capacity was found to be about 119.5 mAh g^{-1}.

In this paper we have reported the structural and electrochemical properties of $LiMn_{1.5}Ni_{0.4}Cr_{0.1}O_4$ cathode material. We also have investigated its electrochemical behavior for high energy density applications at higher *C* rate.

2. Experimental

Lithium acetate dihydrate [$Li(CH_3COO)\cdot 2H_2O$, 99%], manganese(II) acetate tetrahydrate [$Mn(CH3COO)_2\cdot 4H_2O$, Mn 22%], nickel (II) acetate tetra hydrate [$Ni(CH_3COO)_2\cdot 4H_2O$], and chromium acetate hydroxide (Cr 24%) [$Cr_3(OH)_2(OOCCH_3)_7$] (all produced from Alfa Aesar, USA) were used as a precursor materials. All precursor materials were dissolved separately in 2-ethyl hexanoic acid at 80 °C. After complete dissolution of the precursor materials, all of the solutions were mixed together, followed by heating at 80 °C and stirring for about 1 h. The final solution was then dried to obtain powder. The organic removal from the synthesized powder was carried out by heating the obtained powder at 450 °C for 4 h. After the complete organic removal the material was calcined at 875 °C for 24 h in an oxygen atmosphere, to obtained phase pure $LiMn_{1.5}Ni_{0.4}Cr_{0.1}O_4$ cathode material. The phase purity and the crystallinity of the $LiMn_{1.5}Ni_{0.4}Cr_{0.1}O_4$ cathode material were obtained using a Siemens D5000 X-ray powder diffractometer [Cu Kα radiation, 1.5405 Å]. The cathode was prepared by mixing calcined powder ($LiMn_{1.5}Ni_{0.4}Cr_{0.1}O_4$), carbon black, and polyvinylidene fluoride (weight ratio 80:10:10), and subsequently a slurry was made with *n*-methyl pyrolidone. The resulting paste was cast uniformly onto aluminum foil followed by drying at about 60 °C in an oven overnight. The compositions of the electrode were analyzed using energy-dispersive analysis by X-ray (EDAX). X-ray photoelectron spectroscopy (XPS) measurements of $LiMn_{1.5}Ni_{0.4}Cr_{0.1}O_4$ cathodes were performed before and after charge–discharge cycle, using PHI ESCA system (Physical Electronics) using Al Kα radiation. Curve fitting of the slow-scanned XPS spectra was carried out using a non-linear least-squares fitting program with a Gaussian–Lorentz sum function. The coin cells were fabricated in an argon atmosphere, inside a Glove Box (MBraun Inc., USA), using $LiMn_{1.5}Ni_{0.4}Cr_{0.1}O_4$electrode as cathode, Li foil as anode, and 1 M lithium hexafluoride ($LiPF_6$), dissolved in ethyl carbonate (EC) and dimethyl carbonate (DMC) [1:2, v/v ratio] as electrolyte. The electrochemical behavior of the cells was studied at room temperature by cyclic voltammetry and charge–discharge characteristics, using Solartron battery tester, Model 1470E. The impedance measurements of the cells were carried out using Gamry Instruments potentiostat and EIS 300 electrochemical software.

3. Results and discussions

Fig. 1 shows the XRD pattern of $LiMn_{1.5}Ni_{0.4}Cr_{0.1}O_4$ cathode material, calcined at 875 °C for 24 h in an oxygen atmosphere. All peaks were found corresponding to *Fd*3*m* spinel crystal structure. The XRD pattern showed very intense peaks corresponding to (1 1 1), (3 1 1), and (4 0 0) planes, that indicates the well crystalline

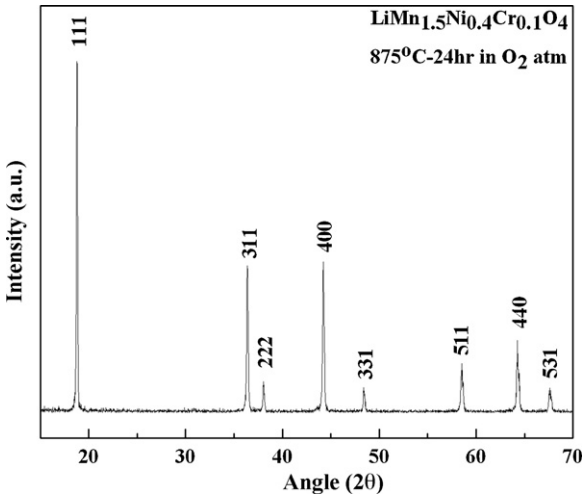

Fig. 1. Powder diffraction patterns of $LiMn_{1.5}Ni_{0.4}Cr_{0.1}O_4$ cathode material, annealed at 875 °C for 24 h in O_2 atmosphere.

nature of the material and the occupancy of Li ions in tetrahedral (8*a*) sites. The manganese, chromium and nickel ions occupy octahedral (16*d*) sites and O^{2-} reside at the general positions (32*e*) [15]. The lattice parameter of $LiMn_{1.5}Ni_{0.4}Cr_{0.1}O_4$ cathode material was obtained using interactive powder diffraction data interpretation and indexing program POWDMULT [16] and was found as 8.1835 Å. The unit cell volume and the standard deviation were found as 548.04 $Å^3$ and 0.00206 $Å^3$, respectively. The lattice parameter of $LiMn_{1.5}Ni_{0.4}Cr_{0.1}O_4$ cathode material was less than that of the lattice parameter of pure $LiMn_2O_4$ (8.247 Å) [17], and $LiMn_{1.5}Ni_{0.5}O_4$ cathode materials, because ionic radii of Cr^{3+} (0.615 Å) is less than the ionic radii of Ni^{2+} (0.69 Å), and Mn^{3+} (0.66 Å) resulting strong bonding energy of Cr with oxygen than Mn or Ni [18]. Further, as confirmed by XPS, the doping of Cr^{3+} and Ni^{2+} in $LiMn_2O_4$ results into the formation of Mn^{4+} (ionic radii 0.60 Å) and the bond length of Mn^{4+}–O is less then that of the bond length of Mn^{3+}–O, resulting in decreased lattice parameter.

It can be seen from the EDAX spectra (Fig. 2) of $LiMn_{1.5}Ni_{0.4}Cr_{0.1}O_4$ cathode that there are peaks corresponding to Mn, carbon, oxygen, nickel, chromium, and fluorine and no other impurity peaks were found in the sample. The peak due to Mn, Ni, Cr, and oxygen are from $LiMn_{1.5}Ni_{0.4}Cr_{0.1}O_4$, carbon due to carbon black, and fluorine is due to PVDF binder, present in the cathode.

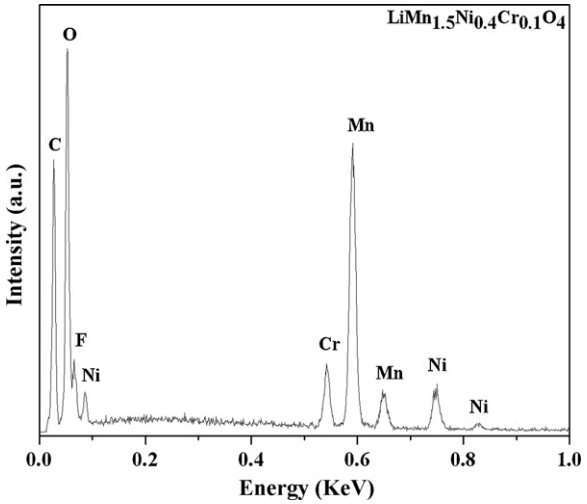

Fig. 2. EDAX spectra of $LiMn_{1.5}Ni_{0.4}Cr_{0.1}O_4$ cathode.

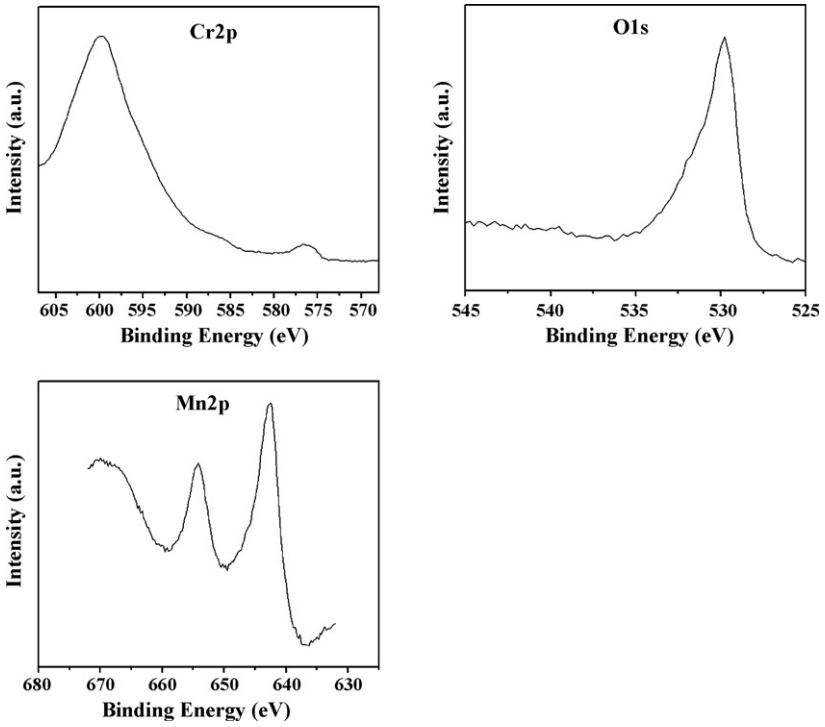

Fig. 3. XPS spectra of $LiMn_{1.5}Ni_{0.4}Cr_{0.1}O_4$ cathode material.

XPS studies of cathode material were carried out to find out the oxidation states of different elements in the material. Fig. 3 shows two peaks in the XPS spectra Mn. The peaks obtained at 641.75 eV and 642.48 eV correspond to Mn^{3+} and Mn^{4+} oxidation states, respectively, and the satellite peak obtained at 654.22 eV is in agreement with the reported one in the literature [12,19,20]. The Cr peak appears at 576.21 eV, indicating that Cr is in 3+ state [9]. The binding energy of O 1s is found to be 529.74 eV.

Cyclic voltammetric studies of $LiMn_{1.5}Ni_{0.4}Cr_{0.1}O_4$ cathode material were carried out in $LiMn_{1.5}Ni_{0.4}Cr_{0.1}O_4/LiPF_6$ + (EC + DMC)/Li coin cells at room temperature and in the voltage range of 3.0–5.0 V at a scan rate of 0.1 mV s^{-1}. The cyclic voltammogram showed [Fig. 4] three well defined oxidation peaks at 4.07 V, 4.76 V, and 4.87 V. The peak at 4.07 V is due to Mn^{3+}/Mn^{4+} redox couple while the peaks at 4.76 V and 4.87 V are due to Ni^{2+}/Ni^{4+} and Cr^{3+}/Cr^{4+} redox couple, respectively [21]. The oxidation peak at 4.87 V indicates that this material can be used for 5 V applications.

The charge–discharge characteristics of $LiMn_{1.5}Ni_{0.4}Cr_{0.1}O_4/LiPF_6$(EC + DMC)/Li coin cells were carried out at room temperature in 3.0–4.9 V range, at various current rate of 0.2*C*, 0.5*C*, and 1*C*, where $C = 147\ mAh\ g^{-1}$. Fig. 5 showed the charge–discharge behavior of $LiMn_{1.5}Ni_{0.4}Cr_{0.1}O_4/LiPF_6$(EC + DMC)/Li coin cells at a constant charge–discharge rate of 0.2*C*. It can be seen from the figure that the initial discharge capacity was 108 mAh g^{-1}, which increases gradually up to 10th consecutive charge–discharge cycles and reached at a maximum value of 126 mAh g^{-1}. The initial discharge capacity increases in the first few cycles that may be due to electrochemical activation of the cathode and improved Li ion diffusion channels in the material, resulting in higher lithium utilization during initial cycling stage [22]. The

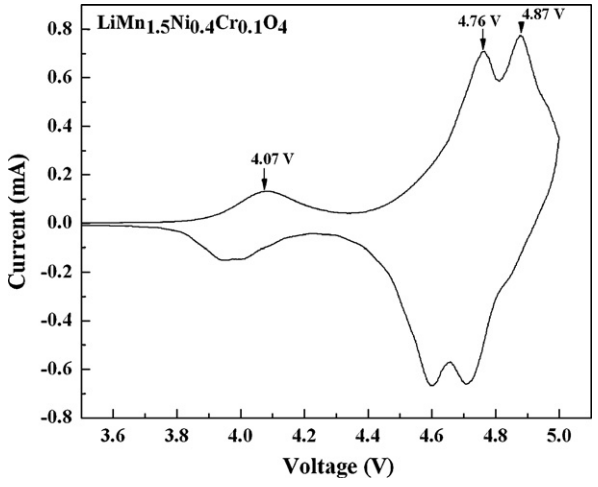

Fig. 4. Cyclic voltammogram of $LiMn_{1.5}Ni_{0.4}Cr_{0.1}O_4/LiPF_6$ + (EC + DMC)/Li coin cell in 3.0–5.0 V range, at a voltage scan rate of 0.1 mV s^{-1}.

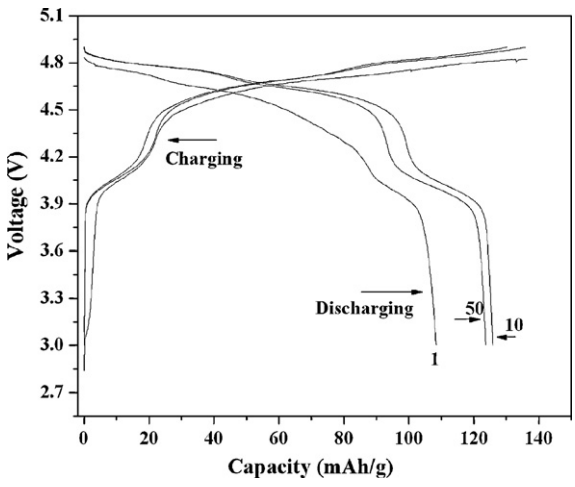

Fig. 5. Room temperature charge–discharge behavior of $LiMn_{1.5}Ni_{0.4}Cr_{0.1}O_4/LiPF_6$ + (EC + DMC)/Li coin cell in 3.0–4.9 V range at a constant current rate of *C*/5.

Table 1
Comparison between the cyclic performance of our cathode materials and the reported earlier works.

S. No.	Material	Voltage range (V)	Charge–discharge *C* rate	Maximum/initial discharge capacity	No. of cycle	Discharge capacity retention (%)	Refs.
1	$LiCr_{0.5}Mn_{1.5}O_4$	3.5–5.0	0.65 mA cm^{-2}	140	4	138.6	[9]
2	$LiMn_{1.95}Cr_{0.05}O_4$	3.0–4.5	0.1 mA	130	30	91	[24]
3	$LiMn_{1.9}Cr_{0.1}O_4$	2.5–4.8	0.1*C*	138	10	100	[25]
4	$LiMn_{1.4}Cr_{0.2}Ni_{0.3}O_4$	3.3–4.95	0.15*C*	130.8	50	94.1	[14]
5	$LiMn_{1.4}Cr_{0.6}O_4$	3.0–5.0	0.1*C*	142	1	–	[13]
6	$LiMn_{1.9}Cr_{0.1}O_4$	2.5–4.8	0.1*C*	139	10	88	[26]
7	$LiMn_{1.5}Ni_{0.4}Cr_{0.1}O_4$	3.0–4.9	0.2*C*	126	50	98.5	Present work
			0.5*C*	110	50	97.2	
			1*C*	100	50	96	

electrode showed stable behavior upon cycling and after 50 charge–discharge cycles the discharge capacity was found to be about 123.7 mAh g^{-1}.

Fig. 6 shows the cycleability of $LiMn_{1.5}Ni_{0.4}Cr_{0.1}O_4$/$LiPF_6$(EC + DMC)/Li coin cells at various *C* rates (1*C*, 0.5*C*, and 0.2*C*). The maximum discharge capacities at 1*C*, 0.5*C*, and 0.2*C* current were found to be about 100 mAh g^{-1}, 110 mAh g^{-1}, and 126 mAh g^{-1}, respectively. The discharge capacity retentions were found as 98.5%, 97.2%, and 96% after 50 charge–discharge cycles at the discharge current rates of 0.2*C*, 0.5*C*, and 1*C*, respectively. In the Table 1 we have presented a comparison between the cyclic performance of $LiMn_{1.5}Ni_{0.4}Cr_{0.1}O_4$ cathode materials, synthesized by us and those reported earlier by various researchers. It can be seen from Table 1 that $LiMn_{1.5}Ni_{0.4}Cr_{0.1}O_4$ could be a promising cathode material for high rate capability applications.

Fig. 7 shows the impedance spectra of $LiMn_{1.5}Ni_{0.4}Cr_{0.1}O_4$/$LiPF_6$ + (EC + DMC)/Li coin cell before and after charge–discharge cycles The impedance spectra were obtained within the frequency range of 10 mHz to 1 MHz. It can be seen from the figure that the charge-transfer resistance does not change upon cycling. Before and after charge–discharge cycles, the charge-transfer resistance was found to be about 78 Ω, indicating that there is no SEI layer formation on the surface of cathode after charge–discharge cycling, which is the main cause of stable behavior of the cells. The slope of the inclined line at low frequency region is almost the same, indicating that the Werburg impedance in the low frequency region does not change, confirming that there is no change in Li^+ activity upon cycling [23].

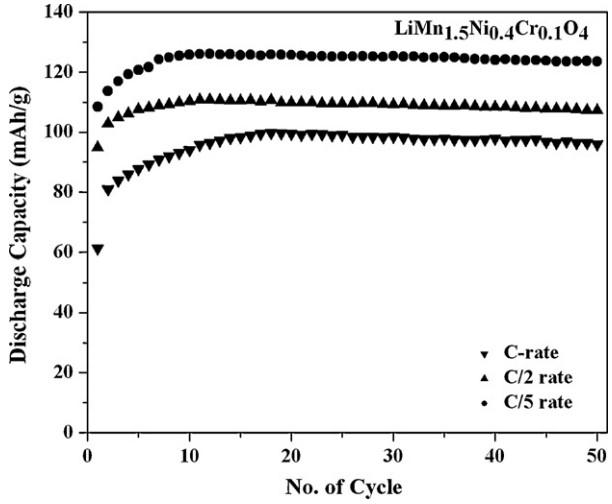

Fig. 6. Cyclability of $LiMn_{1.5}Ni_{0.4}Cr_{0.1}O_4$/$LiPF_6$ + (EC + DMC)/Li coin cell. The cell was charge and discharged in cell in 3.0–4.9 V range at a constant current rates of *C*, *C*/2, and *C*/5.

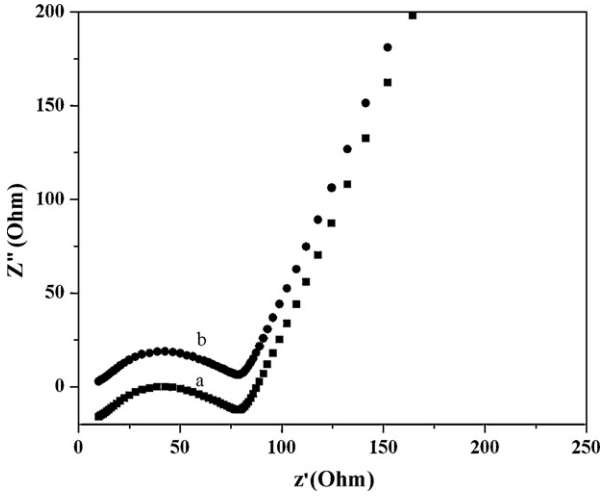

Fig. 7. Impedance spectra of $LiMn_{1.5}Ni_{0.4}Cr_{0.1}O_4$/$LiPF_6$ + (EC + DMC)/Li coin cell: (a) before charge–discharge and (b) after 50 charge–discharge cycles.

4. Conclusions

We have synthesized phase pure $LiMn_{1.5}Ni_{0.4}Cr_{0.1}O_4$ cathode material by sol–gel method. The XRD data of the above materials showed cubic spinel network (*Fd*3*m*). The redox voltage peaks in the cyclic voltammogram showed the reversible reactions involved in Li ion intercalation and de-intercalation in the structure. The charge–discharge characteristics at various *C* rate showed the stable behavior of $LiMn_{1.5}Ni_{0.4}Cr_{0.1}O_4$ cathode materials, even at higher *C* rate of 1*C*, indicating that this material could be used as high energy density and high rate capability cathode material for Li ion rechargeable batteries. Further investigations are in progress in order to improve the discharge capacity of $LiMn_{1.5}Ni_{0.4}Cr_{0.1}O_4$ cathode material by surface modifications with ZnO, Al_2O_3, and ZrO_2.

Acknowledgements

The authors gratefully acknowledge partial support by the NASA grant NNX08AB12A and NNX08BA48A for this research work. The XRD and EDAX measurements were carried out utilizing Materials Characterization Center (MCC) facilities at UPR.

References

[1] S.J. Kim, S.H. Kim, D.H. Kim, J.S. Im, H.Y. Ahn, J.W. Kang, E.J. Kim, J. Kim, Phys. Scr. T129 (2007) 57.
[2] J.C. Arrebola, A. Caballero, L. Hernan, J. Morales, J. Power Sources 183 (2008) 310.
[3] S. Patoux, L. Sannier, H. Lignier, Y. Reynier, C. Bourbon, S. Jouanneau, F.L. Cras, S. Martinet, Electrochim. Acta 53 (2008) 4137.

[4] Q. Zhong, A. Bonakdarpour, M. Zhang, Y. Gao, J.R. Dahn, J. Electrochem. Soc. 144 (1997) 205.
[5] R.I. Eglitis, G. Borstel, Phys. Stat. Sol. (a) 202 (2005) R13.
[6] Y. Xia, Y. Zhou, M. Yoshio, J. Electrochem. Soc. 144 (1997) 2593.
[7] D.H. Jang, J.Y. Shin, S.M. Oh, J. Electrochem. Soc. 143 (1996) 2204.
[8] R.J. Gummow, A. Dckock, M.M. Thackeray, Solid State Ionics 69 (1994) 59.
[9] Y.K. Yoon, C.W. Park, H.Y. Ahn, D.H. Kim, Y.S. Lee, J. Kim, J. Phys. Chem. Solids 68 (2007) 780.
[10] Y. Wei, K.B. Kim, G. Chen, Electrochim. Acta. 51 (2006) 3365.
[11] R. Singhal, J.J.S. Aries, R. Katiyar, Y. Ishikawa, M.J. Vilkas, S.R. Das, M.S. Tomar, R.S. Katiyar, J. Renew. Sustain. Energy 1 (2009) 023102.
[12] S. Rajakumar, R. Thirunakaran, S. Sivashanmugam, J.I. Yamaki, S. Gopukumar, J. Electrochem. Soc. 156 (2009) A246.
[13] K. Suryakala, G.P. Kalaignan, T. Vasudevan, Mater. Chem. Phys. 104 (2007) 479.
[14] T.F. Yi, J. Shu, Y.R. Zhu, R.S. Zhu, J. Phys. Chem. Solids 70 (2009) 153.
[15] M.M. Thackeray, W.I.F. David, P.G. Bruce, J.B. Goodenough, Mater. Res. Bull. 18 (1983) 461.
[16] E. Wu, POWDMULT, version 2.1, An Interactive Powder Diffraction Data Interpretation and Indexing Program, School of Physical Science, Flinders University of South Australia, Bedford Park, South Australia 5042.
[17] S.J. Bao, Y.Y. Liang, H.L. Li, Mater. Lett. 59 (2005) 3761.
[18] S.B. Park, W.S. Eom, W.I. Cho, H. Jang, J. Power Sources 159 (2006) 679.
[19] Q.H. Wu, J.M. Xu, Q.C. Zhuang, S.G. Sun, Solid State Ionics 177 (2006) 1483.
[20] K.M. Shaju, G.V. Subba Rao, B.V.R. Chowdari, Solid State Ionics 152–153 (2002) 60.
[21] M. Aklaloucha, J.M. Amarillaa, R.M. Rojas, I. Saadoune, J.M. Rojo, J. Power Sources 185 (2008) 501.
[22] X.X. Xu, J. Yang, Y.Q. Wang, Y.N. NuLi, J.L. Wang, J. Power Sources 174 (2007) 1113.
[23] I.S. Jeong, J.U. Kim, H.B. Gu, J. Power Sources 102 (2001) 55.
[24] Y.P. Fu, Y.H. Su, C.H. Lin, J. Power Sources 166 (2004) 137.
[25] R. Thirunakaran, A. Sivashanmugam, S. Gopukumar, C.W. Dunnill, D.H. Gregory, Mater. Res. Bull. 43 (2008) 2119.
[26] R. Thirunakaran, A. Sivashanmugam, S. Gopukumar, C.W. Dunnill, D.H. Gregory, J. Mater. Process. Technol. 208 (2008) 520.